IEJ
Iranian Endodontic Journal

Anatomic Two-dimensional and Three-dimensional Models for Cyclic Fatigue Testing of Endodontic Instruments

Lucila Piasecki [a*], **Steven Robert Makowka** [b], **Gianluca Gambarini** [c]

a Department of Periodontics and Endodontics, University at Buffalo, Buffalo, New York, USA; b Department of Restorative Dentistry, University at Buffalo, Buffalo, New York, USA; c Department of Endodontics, Sapienza University, Rome, Italy

ARTICLE INFO

Article Type: **Original Article**

Received: 08 Nov 2019
Revised: 03 Feb 2020
Accepted: 19 Feb 2020
Doi: *10.22037/iej.v15i2.27342*

**Corresponding author*: Lucila Piasecki, Department of Periodontics & Endodontics, University at Buffalo, 240 Squire Hall, Buffalo NY 14214 USA.

Tel: +1-716 8296197
E-mail: lucilapi@buffalo.edu

ABSTRACT

Introduction: In this study, new devices were developed and evaluated for cyclic fatigue testing (CTF) of endodontic instruments in two-dimensional (2D) and three-dimensional (3D) replicas of the internal anatomy of a mesial root of a mandibular molar. **Methods and Materials:** The trajectories of both curved mesial canals of the same root were outlined from computed tomographic scans and exported to a computer assisted drawing (CAD) software. In the CAD program, the canals were virtually enlarged to a size 25/0.06. The CTF devices were then prototyped in stainless steel. The 2D models represented the bucco-lingual (BL) and mesio-distal (MD) views of the canals, while the original trajectory was kept in the 3D model. Vortex Blue 25/0.06 instruments were tested for fatigue in the six canals (n=12). The number of cycles to failure (NCF) and fragment length (mm) were recorded. Data was statistically analyzed (ANOVA and post-hoc Games-Howell test) with the level of significance set at 5%. **Results:** The mean NCF was significantly different among all the canals (P<0.05). The lifespan of the files was greater in the 2D-BL models, followed by the 2D-MD and 3D. The mean fragment length was also different among the tested models (P<0.05). **Conclusions:** The tested 2D and 3D representations of the same canal trajectory resulted in significant differences both in the amount of stress (seen from NCF) and localization of the maximum stress (seen from fragment length). Further investigations are required to better understand the effects of different 3D curvatures on the cyclic fatigue of endodontic instruments.

Keywords: Cyclic Fatigue; Dental Instruments; Endodontics; Nickel-Titanium

Introduction

Cyclic fatigue tests are currently the most widely used *in vitro* test to evaluate the resistance to breakage of endodontic instruments. However, to date there is no specification or international standard for cyclic fatigue tests. Different methods and several various devices have been described in the literature, thus preventing accurate comparison between some of the studies [1-4]

The design of the canal curvature is considered to be the most crucial factor in determining the results of cyclic fatigue tests. Currently, most cyclic fatigue testing devices are constructed by using Pruett's criteria, with curvatures defined by their angle, radius and distance from the tip of the instrument [2, 3, 5, 6]. In the majority of studies, only a single curvature was included in the artificial canal. The rationale for this choice was to have a precise geometrical model focused on the analysis of only one specific factor or variable. It has been demonstrated that the resistance to fatigue of endodontic instruments decreases as the severity of the angle and radius of the curvature increases [2, 3, 5, 7] , and is additionally affected by the position of the bending stress [4, 8]. More recently, it has been shown that the presence of double-curved (S-shaped) canals also decreases the lifespan of the endodontic instruments [9-12].

The use of different artificial root canals presenting variations in the curvatures has been very useful in the investigation of some aspects of the mechanical behavior of endodontic instruments. However, the manufactured curvatures of all these cyclic fatigue devices are derived from a theoretical geometrical analysis impairing the correlation with the anatomy clinically visualized in radiographs [1, 6, 7, 13].

The internal anatomy of the teeth and the configuration of the root canals is highly variable, and very different from the geometrical designs of the previously mentioned cyclic fatigue devices [14-16]. Moreover, multiple curvatures are very common in posterior teeth and they usually occur in different planes [15, 17, 18] dissimilar from the previously described S-shaped artificial canals [1, 9, 11, 13]. In a natural tooth, the curvatures are three-dimensional, and might result in a more complex and possibly more challenging configuration [18]. cone-beam computed tomography (CBCT) study has shown that mesial roots of mandubular molars presented with A greater number of curvatures, and were of higher complexity when visualized in a proximal view versus a clinical view [15]. Nevertheless, the relevance of real three-dimensional anatomical trajectories on the cyclic fatigue resistance of endodontic instruments has never been reported.

Therefore, the aim of the present study is to introduce new devices for cyclic fatigue testing. These devices are manufactured with the aid of computer guided technology to create two-dimensional and three-dimensional models presenting artificial canals which are replicas of the anatomy of a mesial root of a mandibular molar, in order to assess the effect that these anatomical trajectories have on the resistance of endodontic instruments. The null hypotheses was that the resistance to cyclic fatigue will not be affected by the use of different models of the same canal.

Materials and Methods

Development of the models

CBCT data used for the development of the current models was collected from our previous study [15]. CBCT scans had been taken using the GXDP-500 system (Gendex Dental, Biberach, Germany), operating at 90 kVp and 7 mA, with an exposure time of 23 sec and a voxel size of 0.2 mm^3, with a field of view of 13×13 cm, allowing measurements to an accuracy of 0.2 mm. Out of the 100 mandibular molars from the aforementioned study, three teeth with the following representative anatomy were selected: mesial root with two confluent canals (Vertucci type II), in which one curvature in the bucco-lingual (BL) view was observed and 2 curvatures in the mesio-distal (MD) view. Additionally, the teeth had mature apices, no previous endodontic treatment and no signs of root resorption.

The trajectories of the root canals were outlined using the tools of the software 3D Endo™ (Dentsply Sirona, Wels bei Salzburg, Austria). Briefly, the CBCT scans were analyzed by an experienced operator to detect the orifice and apical foramen of the canals. The automated pathway provided by the software was adjusted to be centered along the entire canal in three-dimensions. The mesio-buccal (MB) canal was colored in blue and the mesio-lingual (ML) canal in green (Figure 1A).

The information regarding the trajectories of the mesial canals were exported to CAD (computer assisted drawing) software for manipulation and part design (Autodesk Inventor 2017; Autodesk, San Rafael, CA, USA). The position and angles of the curvatures were recorded and kept constant (Figures 1B and 1C). Then, the shape of the canals was modified to fit the dimensions of a 25/0.06 endodontic instrument with 18 mm length, and increased of 0.2 mm to allow the free rotation of the files [2]. After enlarging the dimensions, it was observed that in two cases the trajectory of ML and MB canals were overlapping because of the proximity of the canals. Therefore, for these two teeth it was not possible to develop the three-dimensional (3D) models and they were excluded.

The final design of the remaining tooth was used to generate the two-dimensional (2D) models that corresponded to both BL and MD views of each root. The 2D canals were incorporated into a bounding box of small dimensions (10mm×4mm×0.5mm). Table 1 presents the angles and radii of curvature of the artificial canals of the models.

Table 1. Angles and radii of the curvatures in the 2D cyclic fatigue model

	Coronal curve			Apical Curve		
	Angle (°)	**Radius (mm)**	**Distance to the tip (mm)**	**Angle (°)**	**Radius (mm)**	**Distance to the tip (mm)**
Canal MB 2D-BL	45.27	12.5	12.89	20.98	21.73	4.023
Canal MB 2D-MD	84.42	8.95	11.87	42.4	7.15	2.65
Canal ML 2D-BL	20.9	17.93	14.01	32.53	18.93	5.37
Canal ML 2D-MD	39.12	6.14	13.39	18.6	24	6.1

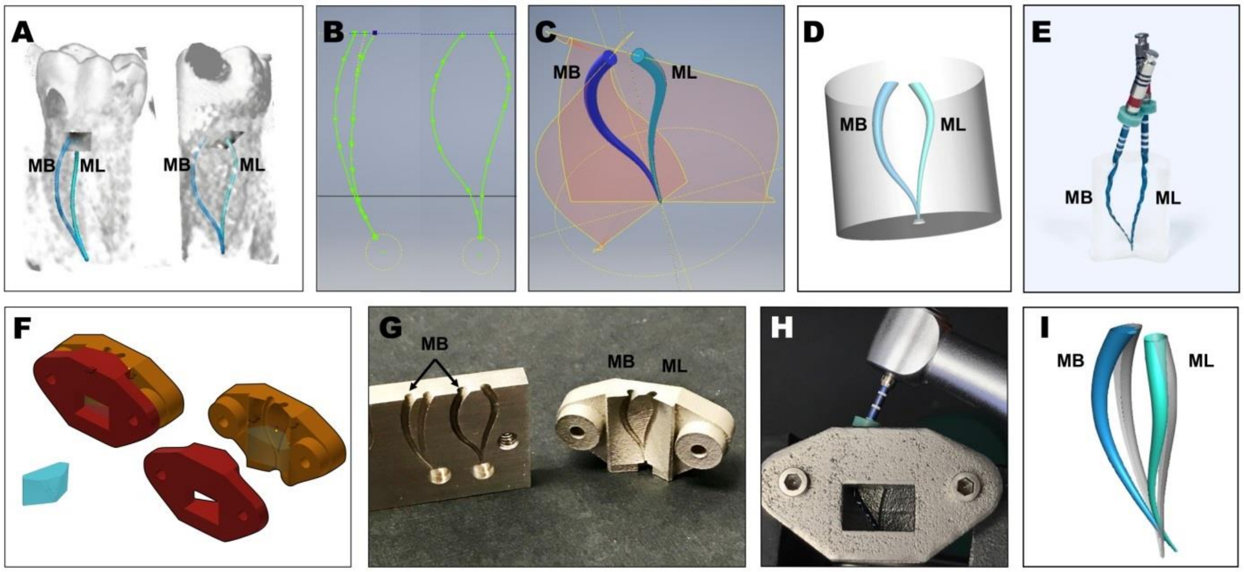

Figure 1. *A*) The rendering of CBCT images of the mandibular molar and the pathways of the canals displayed in a bucco-lingual (right) and mesio-distal (left) views using the software 3D Endo; *B* & *C*) The canal trajectories exported to CAD software to create the 2D and 3D models; *D* & *E*) The 3D canals were included in a virtual cylinder was prototyped in acrylic transparent resin to check the fit of the Vortex Blue 25.06 files; *F*) The final virtual design of the 3D model, presenting two halves and a small window; *G*) The 2D and 3D models prototype d in stainless steel; *H*) Cyclic fatigue testing is shown in the canal MB of the 3D model; *I*) Superimposition of the virtual 2D-MD and 3D canals can be seen

The 3D canals were encompassed by a virtual cylinder (Figure 1D) which was at first prototyped in acrylic resin to check the fit of the instruments (Figure 1E). The final design model consists of two metal halves that can be mated together and attached with screws (Figure 1F). Each of these halves contains a longitudinal profile of the canal, with the bottom half containing most of the perimeter of the canal (about 70% of the circumference) (Figure 1G). The top half contains a window printed in transparent polymer to allow the visualization of the middle third of the canal (Figure 1F).

The 2D and 3D models were exported as a stereo lithography file (STL) and printed in 304 stainless steel with direct metal laser sintering (DMLS) using high-resolution 20 micron layers. The 2D models were manufactured with a 3-axis CNC milling machine (Figure 1G).

Cyclic fatigue test

Ninety Vortex Blue nickel-titanium endodontic instruments (Dentsply Tulsa Dental Specialties) taper 25/0.06 and size 25 were selected for the study. All instruments were initially observed with a stereomicroscope under 20× (Karl Kaps Gmbh, Asslar, Germany) to discard those with visible deformations or defects. The instruments were randomly divided into six groups (*n*=15) to be tested in the different versions (2D-BL, 2D-MD, and 3D) of the MB and ML canals.

Similar to previous studies [2, 10, 19], a main frame was used to hold the block containing the artificial canals, and to allow a precise and reproducible positioning of the instruments. The endodontic handpiece was connected to a 360º rotating bench vise that allowed the instruments to follow the three-dimensional inclination of the canals (Figure 1H). The setting was kept constant, allowing the precise and reproducible placement of the instruments to the same position inside the artificial canals. The entire length of the instruments were precisely fited to the stainless-steel artificial canals. Synthetic oil was used as a lubricant to reduce friction between the metal instruments and the walls of the artificial metal canal. Instruments were rotated until fracture using a conventional electronic endodontic motor set at 500 rpm. The files were observed through a transparent acrylic cover (2D model) or window (3D model).

The time to fracture was recorded in seconds, using both a 1/100-s digital chronometer and a digital camera. The timing was stopped when the fracture of the file was detected visually and/or audibly; the failure was then confirmed in the video recording with a precision of 1/100 of a second. If no breakage occurred after 10 min, the rotation was stopped. The length of the fractured tip of each instrument was measured to a precision of 0.01 mm with a digital caliper.

Statistical analysis

The data of the time to fracture and fragment length were statistically analyzed (ANOVA and post-hoc Games-Howell test) with the significance set at the 95% confidence level, using the SPSS software (SPSS version 20.0, SPSS, Chicago, IL, USA).

Results

The mean and standard deviations for NCF and fragment length are presented in Table 2. No breakage occurred in the files rotated in the canal ML of the 2D-BL model. Data was normally distributed (Shapiro-Wilk's test, $P>0.05$), but only the variable fragment length presented equal variance (Levene's test, $P>0.05$).

The one-way ANOVA (Games-Howell post hoc) showed that there was a statistically significant difference in NCF among all groups ($P<0.05$). The mean fragment length was statistically different among all groups (ANOVA, Tukey HSD, $P<0.05$), except between MB canal comparing the 2D-MD and the 3D model.

Discussion

In the present study, new 2D and 3D devices with artificial canals were developed for fatigue tests which replicate the dental anatomy obtained from CBCT scans of a patient so as to replicate a clinical scenario. Although the developed 2D models are the representations of the same canals in BL and MD views, their trajectories are completely different, which directly impacted the resistance to cyclic fatigue of the tested files. In the 2D-MD model, the canal ML resulted in significantly less cycles compared to the MB canal cycles, while in the BL representation of the same canals, the low stress of the ML canal was not enough to break the files after 5000 cycles (10 min of testing). The increased canal complexity in the bucco-lingual aspect of the roots has been previously stated [15-17], but never before had it been translated into a fatigue device.

Clinical intra-canal fracture of endodontic instruments is related to many factors acting together: bending stresses due to the anatomical complexities of the tooth, torsional stresses related to instruments' cutting ability, debris removal, hardness of dentine as well as the operator- related factors [20-23]. In a laboratory setting, it is not possible to combine all of these conditions, thus the main goal of a cyclic fatigue test is to analyze the resistance to bending stresses within controlled parameters [24-27]. Since the design of the canal curvature plays an important role in determining bending stress, a realistic design similar to *in vivo* curvatures is an improvement that has the potential to increase the clinical relevance of the cyclic fatigue tests [1, 4, 12].

Table 2. Descriptive for the Number of Cycles to Failure (NCF) and Fragment length (mm) (n=12)

	NCF	Fragment length (mm)
	Mean (SD)	Mean (SD)
Canal MB 2D-BL	524 (112.4)[a]	10.04 (0.45)[a]
Canal MB 2D-MD	88 (28.2)[b]	11.75 (0.45)[b]
Canal MB 3D	55 (11.7)[c]	11.33 (0.25)[b, c]
Canal ML 2D-MD	40 (10.1)[d]	10.83 (0.54)[c]
Canal ML 3D	25 (9.8)[e]	14.50 (0.43)[d]

BL, bucco-lingual; MD, mesio-distal; 3D, three-dimensional; Different superscript lowercase letter indicates statistical significance within columns (P<0.05): The fourth line where no failure has occurred is not included in the analysis

The root canal anatomy that was selected for this preliminary study were the mesial canals of the mandibular molar due to its known challenging morphology [15, 16, 18]. The trajectories of the canals were highlighted using the specific tools of the software 3D Endo [15, 28] , and then they were enlarged to fit instruments of size 25/0.06 which corresponds to an average apical size for preparation in curved canals [29, 30]. It has been demonstrated that a good correspondence between the artificial canal and instruments taper is needed to avoid errors related to the possibility of instruments straightening while rotating inside an artificial canal that is too wide [1, 6]. If this happens the results of the cyclic fatigue test can be significantly influenced by an instrument's flexibility, because the curvature the different instruments follow is no longer the same. Vortex Blue instruments were selected because it presents constant taper and cross-section, thus preventing bias related to the design. The 3D model presents a configuration in which the curvatures of both 2D models are combined in a three-dimensional space. Although the 2D-MD canal presents a design that overall is very similar to the 3D configuration, the resistance of the files to fatigue was significantly lower in the latter. The possible explanation is that, although the curves of the BL plane were shallow, they considerably increased the stress load in the 3D model. In the superimposition of the virtual canals of the 2D-MD and 3D models, it is possible to note the spatial difference between these two representations. Notwithstanding, it is important to note that the combination of stress in the three-dimensional space is complex: the determination of the actual angle of curvature should be ascertained with a plane that follows the canal trajectory in all three dimensions [31, 32]. Clinically, this means that the curvatures not seen in the BL view might significantly affect the performance of the instruments. Therefore, assessing the difficulty of a case by only analyzing a periapical radiograph may be misleading. This novel study highlights the importance of a three-dimensional preoperative evaluation of curved canals [14, 15, 17, 31]. Future developments in CBCT software should consider including the automatic measurement of the curvature angles in the 3D space, allowing for a more comprehensive evaluation of the case difficulty [15, 28, 31, 33].

As previously mentioned, the main difference between our anatomical model and the previous geometric artificial canals is related to the design of the curvatures. Most investigations that used geometrical S-shaped artificial canals reported that the file broke first at the apical curvature, which was correlated to its sharper angle [9, 10, 13]. On the other hand, in the present study all the fractures occurred in the coronal curvature: this can be partially explained because the angle and radii were more challenging than the apical curve in the present canals, but also by the location of the bending stress, which was applied in a point of the file presenting larger dimensions [1, 4, 34]. Nevertheless, these results highlight the importance of coronal flaring to decrease the angle of cervical curvatures and consequently the stresses applied to the instruments [18, 33].

In the geometrical models, the factors that may interfere in fatigue resistance have been evaluated individually, such as position, and different radius and degrees of curvature, *etc*. However, the anatomic trajectory not only combines those factors with a variety of angles/radii, but also might present straight parts and curvatures in more than one plane. In the present study, the combination of all these different parameters dictated by the anatomy resulted in a unique bending stress for each canal/model tested. Thus, the results showed a significant difference among the different representations of the same canal trajectory, not only in the amount of stress, but also in the localization of the maximum stress. Although the 3D device seems to be the most realistic model, further investigation is required to better understand the effect of the three-dimensional bending stresses of a given anatomic canal trajectory. Nevertheless, the proposed methodology might be used in future investigations to evaluate different parameters, to plan or simulate the endodontic procedures, and to predict the behavior of instruments and other materials that might be affected by the anatomy [4, 15, 31] .

It is important to note that in this preliminary study, results were obtained from one specific tooth and its relevance is limited by the high anatomical variability. Also, the selection of a different longitudinal CBCT slice to develop the 2D models could have led to different results, because the anatomy varies along the three planes [15, 17, 28, 33]. Ideally, one would want to develop several different models, or to select the most relevant/prevalent anatomy for the canal models. However, the main limitations of the proposed methodology are related to the expertise in CAD design and the costs of the high precision prototyping of the models in stainless steel.

Conclusion

The proposed methodology is a step forward in the development of a more realistic model for cyclic fatigue testing that will potentially help translate *in vitro* results to clinical setting. Also, the preliminary results highlighted the importance of considering the three-dimensional trajectory when evaluating bending stresses and the difficulty of a case. Further investigations are required to better understand the effects of different 3D curvatures on the fatigue of endodontic instruments.

Conflict of Interest: 'None declared'.

References

1. Plotino G, Grande NM, Cordaro M, Testarelli L, Gambarini G. A review of cyclic fatigue testing of nickel-titanium rotary instruments. J Endod. 2009;35(11):1469-76.
2. Plotino G, Grande NM, Cordaro M, Testarelli L, Gambarini G. Measurement of the trajectory of different NiTi rotary instruments in an artificial canal specifically designed for cyclic fatigue tests. Oral Surg Oral Med Oral Pathol Oral Radiol Endod. 2009;108(3):e152-6.
3. Inan U, Aydin C, Tunca YM. Cyclic fatigue of ProTaper rotary nickel-titanium instruments in artificial canals with 2 different radii of curvature. Oral Surg Oral Med Oral Pathol Oral Radiol Endod. 2007;104(6):837-40.
4. Lopes HP, Chiesa WM, Correia NR, de Souza Navegante NC, Elias CN, Moreira EJ, Chiesa BE. Influence of curvature location along an artificial canal on cyclic fatigue of a rotary nickel-titanium endodontic instrument. Oral Surg Oral Med Oral Pathol Oral Radiol Endod. 2011;111(6):792-6.
5. Plotino G, Grande NM, Melo MC, Bahia MG, Testarelli L, Gambarini G. Cyclic fatigue of NiTi rotary instruments in a simulated apical abrupt curvature. Int Endod J. 2010;43(3):226-30.
6. Plotino G, Grande NM, Mazza C, Petrovic R, Testarelli L, Gambarini G. Influence of size and taper of artificial canals on the trajectory of NiTi rotary instruments in cyclic fatigue studies. Oral Surg Oral Med Oral Pathol Oral Radiol Endod. 2010;109(1):e60-6.
7. Pruett JP, Clement DJ, Carnes DL, Jr. Cyclic fatigue testing of nickel-titanium endodontic instruments. J Endod. 1997;23(2):77-85.
8. Necchi S, Taschieri S, Petrini L, Migliavacca F. Mechanical behaviour of nickel-titanium rotary endodontic instruments in simulated clinical conditions: a computational study. Int Endod J. 2008;41(11):939-49.
9. Al-Sudani D, Grande NM, Plotino G, Pompa G, Di Carlo S, Testarelli L, Gambarini G. Cyclic fatigue of nickel-titanium rotary instruments in a double (S-shaped) simulated curvature. J Endod. 2012;38(7):987-9.
10. Gambarini G, Plotino G, Sannino G, Grande NM, Giansiracusa A, Piasecki L, da Silva Neto UX, Al-Sudani D, Testarelli L. Cyclic fatigue of instruments for endodontic glide path. Odontology. 2015;103(1):56-60.
11. Yilmaz K, Uslu G, Gundogar M, Ozyurek T, Grande NM, Plotino G. Cyclic fatigue resistances of several nickel-titanium glide path rotary and reciprocating instruments at body temperature. Int Endod J. 2018;51(8):924-30.

12. Gundogar M, Ozyurek T. Cyclic Fatigue Resistance of OneShape, HyFlex EDM, WaveOne Gold, and Reciproc Blue Nickel-titanium Instruments. J Endod. 2017;43(7):1192-6.
13. Topcuoglu HS, Topcuoglu G, Duzgun S. Resistance to cyclic fatigue of PathFile, ScoutRaCe and ProGlider glide path files in an S-shaped canal. Int Endod J. 2018;51(5):509-14.
14. Nagy CD, Szabo J, Szabo J. A mathematically based classification of root canal curvatures on natural human teeth. J Endod. 1995;21(11):557-60.
15. Gambarini G, Ropini P, Piasecki L, Costantini R, Carneiro E, Testarelli L, Dummer PMH. A preliminary assessment of a new dedicated endodontic software for use with CBCT images to evaluate the canal complexity of mandibular molars. Int Endod J. 2018;51(3):259-68.
16. Ordinola-Zapata R, Bramante CM, Versiani MA, Moldauer BI, Topham G, Gutmann JL, Nunez A, Duarte MA, Abella F. Comparative accuracy of the Clearing Technique, CBCT and Micro-CT methods in studying the mesial root canal configuration of mandibular first molars. Int Endod J. 2017;50(1):90-6.
17. Cunningham CJ, Senia ES. A three-dimensional study of canal curvatures in the mesial roots of mandibular molars. J Endod. 1992;18(6):294-300.
18. Gu Y, Lu Q, Wang P, Ni L. Root canal morphology of permanent three-rooted mandibular first molars: Part II--measurement of root canal curvatures. J Endod. 2010;36(8):1341-6.
19. Piasecki L, Al-Sudani D, Rubini AG, Sannino G, Bossu M, Testarelli L, Di Giorgio R, da Silva-Neto UX, Brandao CG, Gambarini G. Mechanical resistance of carbon and stainless steel hand instruments used in a reciprocating handpiece. Ann Stomatol (Roma). 2013;4(3-4):259-62.
20. Plotino G, Grande NM, Sorci E, Malagnino VA, Somma F. Influence of a brushing working motion on the fatigue life of NiTi rotary instruments. Int Endod J. 2007;40(1):45-51.
21. Parashos P, Gordon I, Messer HH. Factors influencing defects of rotary nickel-titanium endodontic instruments after clinical use. J Endod. 2004;30(10):722-5.
22. Alapati SB, Brantley WA, Svec TA, Powers JM, Nusstein JM, Daehn GS. SEM observations of nickel-titanium rotary endodontic instruments that fractured during clinical Use. J Endod. 2005;31(1):40-3.
23. Gambarini G, Piasecki L, Di Nardo D, Miccoli G, Di Giorgio G, Carneiro E, Al-Sudani D, Testarelli L. Incidence of Deformation and Fracture of Twisted File Adaptive Instruments after Repeated Clinical Use. J Oral Maxillofac Res. 2016;7(4):e5.
24. Tanomaru-Filho M, Galletti Espir C, Carolina Vencao A, Macedo-Serrano N, Camilo-Pinto J, Guerreiro-Tanomaru J. Cyclic Fatigue Resistance of Heat-Treated Nickel-Titanium Instruments. Iran Endod J. 2018;13(3):312-7.
25. de Menezes S, Machado Batista S, Brandao de Magalhaes DF, Diana Santana A, de Melo Monteiro GQ. Cyclic Fatigue Resistance of Mtwo Rotary Instruments with two Different Instrumentation Techniques. Iran Endod J. 2018;13(1):114-9.
26. Nabavizadeh MR, Sedigh-Shams M, Abdolrasoulnia S. Cyclic Fatigue Life of Two Single File Engine-Driven Systems in Simulated Curved Canals. Iran Endod J. 2018;13(1):61-5.
27. de Menezes S, Batista SM, Lira JOP, de Melo Monteiro GQ. Cyclic Fatigue Resistance of WaveOne Gold, ProDesign R and ProDesign Logic Files in Curved Canals In Vitro. Iran Endod J. 2017;12(4):468-73.
28. Segato AVK, Piasecki L, Felipe Iparraguirre Nunovero M, da Silva Neto UX, Westphalen VPD, Gambarini G, Carneiro E. The Accuracy of a New Cone-beam Computed Tomographic Software in the Preoperative Working Length Determination Ex Vivo. J Endod. 2018;44(6):1024-9.
29. Peters OA, Arias A, Paque F. A Micro-computed Tomographic Assessment of Root Canal Preparation with a Novel Instrument, TRUShape, in Mesial Roots of Mandibular Molars. J Endod. 2015;41(9):1545-50.
30. ElAyouti A, Hulber JM, Judenhofer MS, Connert T, Mannheim JG, Lost C, Pichler BJ, von Ohle C. Apical constriction: location and dimensions in molars-a micro-computed tomography study. J Endod. 2014;40(8):1095-9.
31. Dobo-Nagy C, Keszthelyi G, Szabo J, Sulyok P, Ledeczky G, Szabo J. A computerized method for mathematical description of three-dimensional root canal axis. J Endod. 2000;26(11):639-43.
32. Benyo B, Szilagyi L, Haidegger T, Kovacs L, Nagy-Dobo C. Detection of the root canal's centerline from dental micro-CT records. Conf Proc IEEE Eng Med Biol Soc. 2009;2009:3517-20.
33. Tchorz JP, Wolgin M, Karygianni L, Vach K, Altenburger MJ. Accuracy of CBCT-based root canal length predetermination using new endodontic planning software compared to measurements performed with an electronic apex locator ex vivo. Int J Comput Dent. 2018;21(4):323-8.
34. Azim AA, Tarrosh M, Azim KA, Piasecki L. Comparison between Single-file Rotary Systems: Part 2-The Effect of Length of the Instrument Subjected to Cyclic Loading on Cyclic Fatigue Resistance. J Endod. 2018;44(12):1837-42.

Please cite this paper as: Piasecki L, Makowka SR, Gambarini G. Anatomic Two-dimensional and Three-dimensional Models for Cyclic Fatigue Testing of Endodontic Instruments. Iran Endod J. 2020;15(2): 100-5. Doi: 10.22037/iej.v15i2.27324.